# Sailing status recognition to enhance safety awareness and path routing for a commuter ferry

Baiheng Wu, Guoyuan Li, Tongtong Wang, Hans Petter Hildre & Houxiang Zhang

Published online: 10 Apr 2021.

Submit your article to this journal ⬈

Article views: 237

View related articles ⬈

View Crossmark data ⬈

Taylor & Francis
Taylor & Francis Group

🔓 OPEN ACCESS  Check for updates

# Sailing status recognition to enhance safety awareness and path routing for a commuter ferry

Baiheng Wu ⬡, Guoyuan Li ⬡, Tongtong Wang, Hans Petter Hildre ⬡ and Houxiang Zhang ⬡

Department of Ocean Operations and Civil Engineering, Norwegian University of Science and Technology (NTNU), Ålesund, Norway

**ABSTRACT**

This paper suggests a framework about how log data are used to develop a classifier to recognise the sailing status of a commuter ferry, which, in turn, serves as a tool of safety awareness. Several sailing scenarios are defined under the expertise's interpretation based on log data. A classifier is developed by support vector machine algorithm to recognise different scenarios. The classifying precision is getting improved as the database getting larger. Heat maps are drawn statistically to obtain the likelihood site of each sailing status. Contour maps are drawn by interpolation according to heat maps. Based on contour maps, two evaluation items are proposed to reflect the safety level. The safety level term is used for optimising the control. The established classifier has a recognition precision over 96 percent. A path following simulation is executed to verify the effectiveness of the safety level for enhancing sailing safety.

## 1. Introduction

In the last decade, the artificial intelligence has been extensively studied by researchers from different academic fields of interests, and at the same time, it has also attracted practitioners occupied in various industrial fields to put efforts in, e.g. graphical/semantic recognition, autopilot system for automobiles. There have been scholars introducing the artificial intelligence to marine research and applications, but compared with the prosperity in the mentioned fields, this bundle of techniques still draws less attention in the maritime industry. Multiple reasons may account for the current situation. One of them is the artificial intelligence is not yet well studied, which means its performance cannot be guaranteed in real on-board operations, especially in some critical scenarios at high risk. In other words, we cannot substitute the human expertise on-board by an immature technology. Nevertheless, this reason should not prevent the maritime industry from exploring advanced technologies since the pragmatic value will emerge only after substantial and enough research and tests are proceeded. From another respect, it has been statistically stated that human errors have been the dominant factor for causing shipwrecks (Islam et al. 2017; Wiegmann and Shappell 2017). Even though the current progress in artificial intelligence is thought to be ineligible to replace the role of captains, it can at least assist them to avoid making mistakes so that the risk of human errors can be reduced at a large extent. With the rapid development in some minor subjects, including sensor fusion, data mining, and machine learning, constructing an on-board safety awareness system seems to be worth a shot (Elkins et al. 2010). In this paper, we develop

a framework how on-board log data can be utilised to enhance path routing and sailing safety, and to reflect human expertise as well. We also find a realisable application for this framework: commuter ferries with fixed route and certain number of critical operations in a sailing.

Data are necessary to implement artificial intelligence in any fields, including the maritime industry. As the hardware facility cost decreased remarkably in recent years, basic sensors are commonly equipped on most vessels (even the civil ships), which makes log data more accessible to be collected for research aims (Borkowski 2012; Ren et al. 2021). Besides the accessibility of the data, another concern for the data to be credited for further use is the data quality. Since the wrong data can contaminate the database, and thereby affect the performance of the artificial intelligence in a negative way, the data should be collected and selected meticulously. In this respect, human expertise can give sufficient supply. Therefore, it is believed that log data from any successful and safe sailings are with good quality for further utilisation.

Although it is said that on-board log data are getting more accessible, it is still at a small quantity compared with its counterpart in the automotive field. To ensure that enough data can be obtained to establish an intelligent system, we notice the application of commuter ferry which usually travels between two or more designated ports with a fixed sailing route. Repeated sailings guarantee the quantity of log data. Moreover, such type of routes usually contains countable critical operations at certain areas, which makes it possible to develop an algorithm to recognise different sailing status. With the accumulation of data and a proper utilisation of

**CONTACT** Guoyuan Li ✉ guoyuan.li@ntnu.no 🖂 Department of Ocean Operations and Civil Engineering, Norwegian University of Science and Technology (NTNU), Larsgårdsvegen 2, 6009 Ålesund, Norway

them, we can learn the safety laws from the successful experience of human operations.

In this paper, a safety awareness system is designed for the commuter ferry. The system is developed mainly in two stages: designing a classifier to automatically sort the log data; constructing maps which reflect the sailing safety level based on the sorted data. The classifier predicts the sailing status online and the safety awareness can be given in a quantitative way; it is involved in the control loop to optimise the control input for verification.

Although relevant study is not prevalent in the research in maritime fields, such research has been extensively studied in the automobile field and has been applied in reality. Li et al. (2017, 2019a, 2019b, 2020) studied the classification and recognition of driving style and behaviours in different conditions with popular learning algorithm and different experimental methods. Compared with the pattern recognition, the concept of on-board decision support system is more acquainted with the maritime industry, and the safety awareness system developed in this paper can be seen as a component of such an on-board decision support system. There are different ways to develop on-board decision support systems. For example, some scholars build knowledge-based expert systems to support on-board decision (Perera et al. 2012; Calabrese et al. 2012); some use classical and/or novel control theories and tools to improve the manoeuvrability under particular conditions (Pietrzykowski et al. 2010; Nielsen and Jensen 2011); some introduce advanced algorithms to optimise the path planning and navigation (Lazarowska 2012; Simsir et al. 2014; Vettor and Soares 2015; Pietrzykowski et al. 2017); and some use data from automatic identification system (AIS) to support trajectory reconstruction and path following navigation (Zhang et al. 2018; Xu et al. 2019). From another view, such a safety awareness system is within the issue of situation awareness which has attracted researchers to focus on for aiding on-board operation (Chauvin et al. 2008; Nilsson et al. 2008; Fossdal 2018; Li et al. 2019; Nisizaki 2019). However, most research items stay in a conceptual stage without mathematical calculation and applicable data utilisation framework.

The novelty of the work in this paper locates mainly on two points: (1) Using real log data collected from a commuter ferry, instead of the data from simulators or other types of publishable data (AIS data), to analyse the ship manoeuvring status. Log data outperform other sources by directly reflecting captains' navigating behaviours and logics; (2) interpreting the log data by splitting the sailing route into different scenarios with featured particularity, instead of arbitrarily analysing the entire sailing route as a whole. The proposed safety awareness system is verified in a model predictive control loop which has been a popular control algorithm in the research for the auto-piloting car and autonomous vessel (TøNdel et al. 2003; Hagen et al. 2018; Tengesdal et al. 2020).

The paper is organised as follows: Section 2 introduces the proposed method in detail, including data collection and pre-processing, definition of split scenarios, pre-check before applying machine learning algorithm, the design of SVM and how the result can be interpreted by heat maps and

used to assess the safety level; Section 3 illustrates the result in three parts, including the classification result by SVM, the two types of figures demonstrating the classification result, the online testing and the verification in the control loop. At last, a conclusion of the paper is given as a sum and prospect.

## Nomenclature

| | |
|---|---|
| CLF | classifier |
| CRS | cruising (scenario) |
| CVG | converging (scenario) |
| DCK | docking (scenario) |
| DPT | departing (scenario) |
| KDE | kernel density estimation |
| $L$; $L'$ | label set; label set in each binary classifier |
| MPC | model predictive control |
| MSL | mean safety level |
| OH | optimal hyperplane or maximum margin hyperplane |
| $\hat{p}$; $\hat{p}_N$ | estimated density; normalised estimated density |
| RPM | revolutions per minute |
| RSL | receding safety level |
| SL | safety level |
| SVM | support vector machine |
| TRN | turning (scenario) |
| $t$-SNE | $t$-distributed stochastic neighbour embedding |

## 2. Methodology

The framework for sailing status recognition is shown as Figure 1. It includes several key steps: data collection and pre-processing, the design of SVM and its implementation on log data, interpretation of the classification result and its visualisation, and at last, a quantitative evaluation function is proposed to assess the level of sailing safety of the ferry based on the classification result of the accumulated historical log data. The contents included in Figure 1 will be extendedly explained in the following subsections.

### 2.1. Data collection and pre-processing

Log data used in this paper are from a customised commuting route between Trondhjem Biological Station and the berthing port at the estuary of the Nidelva river located in Trondheim, Norway (the white curve in the map in Figure 1 conceptually illustrates the route). The sailings on the commuting route are executed by R/V Gunnerus, a Research and survey Vessel owned by NTNU. The mileage of this commuting route is around 5 kilometres. The vessel is equipped with a 200 kW bow thruster at front for the positioning operation, two 500 kW main azimuth thrusters for the propulsion and course.

The database is constructed by log data from 16 sailings from September 2016 to June 2017 in a traffic-free environment. The sampling frequency of log data is 1 Hz. The information contained by the database can be sorted into three groups: geographical information, ship motions in different degrees of freedom and on-board machinery status. Since the geographical information is distinctly related to different scenarios (which will be defined in a later part), while we want to seek the laws from the ship status itself, items in the
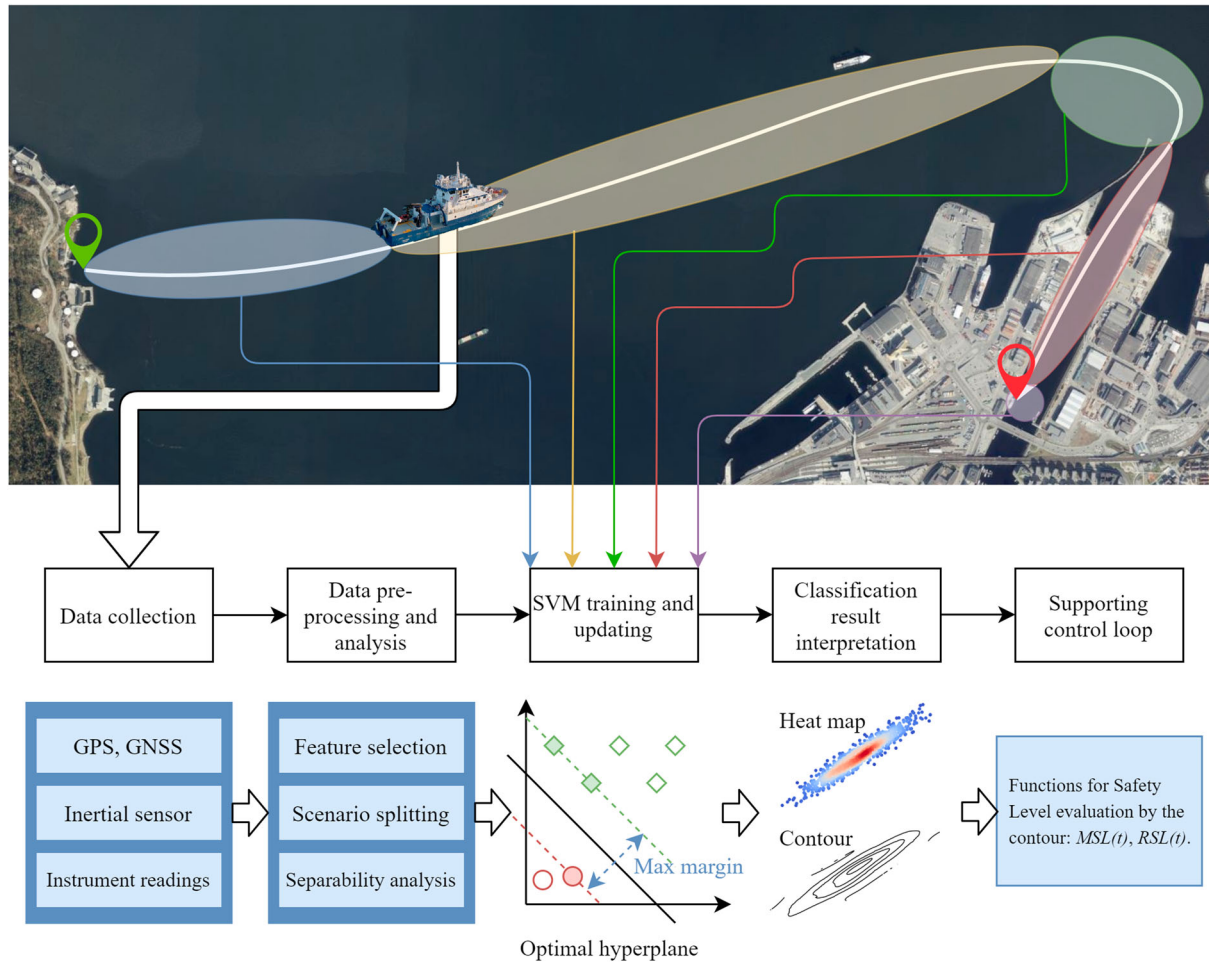
**Figure 1.** Framework of the proposed decision support system for sailing status recognition and safety evaluation (map resource: the Norwegian Mapping Authority). (This figure is available in colour online.)

database reflecting the geographical information are excluded. According to the navigation and manoeuvring habits of captains, featured items are selected from collected data (Wu et al. 2020). They are listed and sorted as in Table 1. All eight featured items in Table 1 are designated as variables for training the scenario recognition algorithm (support vector machine in Section 2.4).

## 2.2. Definition for scenarios by human expertise

According to human expertise, a commuting sailing route can be divided into different scenarios in terms of manoeuvring commands and the vessel response which can be reflected by collected log data. In this customised commuting route, five scenarios are separated from the whole sailing, which are described in detail as follows:

- Departing: the ferry sets off from the port and keeps accelerating.
- Cruising: the ferry usually reaches the rated RPM and travels on the route smoothly.
- Turning: the ferry adjusts its course towards another direction. Deceleration and angular speed increase in this phase.
- Converging: the ferry moves in the narrow channel at a speed lower than the rated, and it finally gets parallel to the coastline with a short distance.
- Docking: the ferry is with no surge speed but only sway, by using the bow thruster to push itself into the berthing point.

The rough illustration of the separation is shown in the map in Figure 1, as five scenarios are marked with ovals in different colours.

Hereupon, the original database is constructed as Equation (1), where $X$ represents for a database consisted of $n$ items described by eight variables mentioned in Table 1.

$$\log \text{data} = \{X; L\}, X \in \mathbb{R}^{n \times 8}, L \in \mathbb{R}^{n \times 1}$$
$$L = \{l_1, l_2, \ldots, l_n\}$$
$$\forall l_i \in L, l_i \in \{\text{departing, cruising, turning, converging, docking}\}$$

**Table 1.** Groups of featured log data items.

| Groups | Ship motion | Machineries |
|---|---|---|
| Data items | Heading (°) | Bow thruster-RPM feedback (%) |
| | Speed (knots) | Port board-RPM feedback (%) |
| | Pitch (°) | Starboard-RPM feedback (%) |
| | | Port board-azimuth feedback (°) |
| | | Starboard-azimuth feedback (°) |

## 2.3. Separability pre-check

Before designing the algorithm for the classifier, it is proper to have a preview of the data to check whether the database is separable. If it is, we may check at a further step to have a sense whether it is linearly separable, approximate linearly separable or not, so that we may determine some properties of the classifier to be designed later.

Firstly, the database is examined by the *t*-distributed stochastic neighbour embedding (*t*-SNE) algorithm (Maaten and Hinton 2008). By the algorithm, the high-dimensional database is converted into a visualisable low-dimensional database:

$$X = \{x_1, x_2, \ldots, x_n\} \in \mathbb{R}^{n \times 8} \xrightarrow{t\text{-SNE}}$$
$$Y = \{y_1, y_2, \ldots, y_n\} \in \mathbb{R}^{n \times 2} \tag{2}$$

The *t*-SNE result is shown as in Figure 2. From the visualised result, it can be clearly found that there is a trend for each scenario to get clustered, hence it can be inferred that the sailing route can be separated into different scenarios based on the selected data.

Besides *t*-SNE, pair plots can be used to reflect the independency of each class. Here, two pair plots are selected and shown in Figure 3. From the self-correlation of port thruster RPM, heading and speed, it shows that there is independency between different scenarios. And bow thruster RPM also gives useful information to tell scenarios apart, e.g. docking data points are explicitly away from other scenarios when the bow thruster is in correlation with port thruster RPM. It should be noted that the power density function (PDF) value of the bow thruster self-correlation at 0 is dominant over the scale. This results from that the bow thruster is strictly kept turned off in almost whole period over scenarios including cruising, turning and converging. While in departing and docking scenarios, the bow thruster is not kept at a fixed running rate, the scattering makes the PDF at each value to be trivial against the counterpart at 0.

Since the database is with a dimensionality at 8, which can be considered as a high dimensional database. From the pre-check of *t*-SNE dimension reduction and the pair plots, we may putatively assume scenarios in the sailing route described by log data are approximate linearly separable.

## 2.4. Support vector machine

SVM algorithm is chosen to build a classifier to solve the classification problem. The SVM algorithm is trained with collected log data according to eight features in Table 1. In practice, we convert the multiclass classification problem into several binary classification problems (Aly 2005). Then, there will be a specific classifier $CLF_k$ for scenario $k$, and 5 in total for all scenarios. Taking scenario $k$ as an example, for the data points whose original labels are the same as scenario $k$, they will be given new labels 1; otherwise, they will be given new labels −1. Then a new vector $L'$ will be created by updated labels, and the vector will substitute the original label $L$. This process can be expressed as follows:

$$CLF_k : \begin{cases} l'_i = 1, & \text{if } l_i = k \\ l'_i = -1, & \text{otherwise} \end{cases} \tag{3}$$

For each binary classifier, there is a specific optimal hyperplane:

$$OH_k : W_k X + b_k = 0 \tag{4}$$

where $W_k$ is the normal vector to the hyperplane. The optimal hyperplane lies between two parallel hyperplanes:

$$OH_k^+ : W_k X + b_k = 1$$
$$OH_k^- : W_k X + b_k = -1 \tag{5}$$

Points on and above hyperplane $OH_k^+$ will be assigned label 1, and finally turns into label $k$. And points on and below hyperplane $OH_k^-$ will be assigned label −1, and finally will not be classified into the dataset of scenario $k$.

While the SVM algorithm is designed, the database is updated after every sailing so that the classifier built by SVM evolves simultaneously. And the updated classifier can be used to recognise the scenario status in subsequent sailings. The idea of this training process is mainly borrowed from
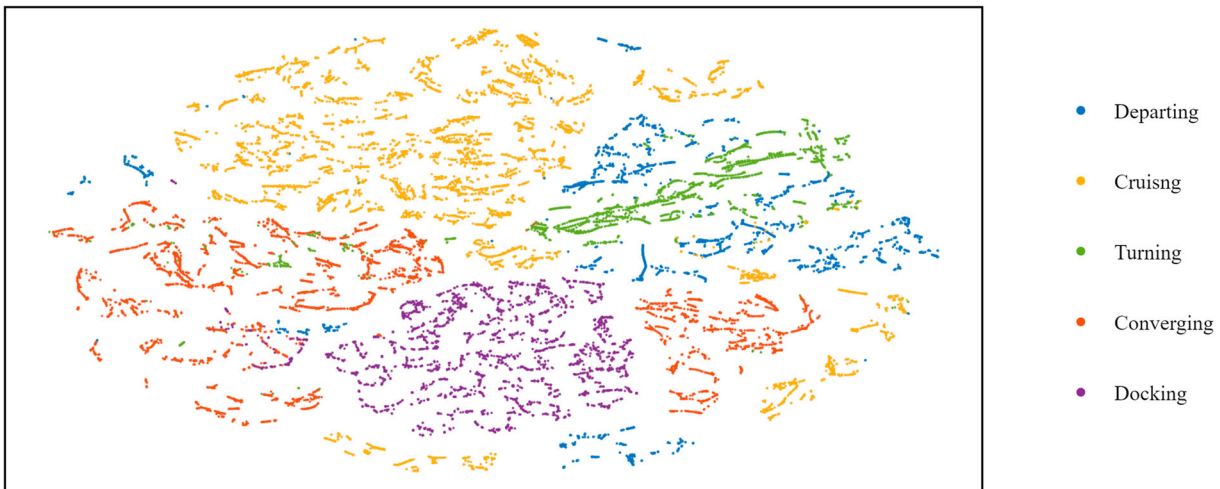


**Figure 2.** Visualisation of dimension reduction result by *t*-SNE. (This figure is available in colour online.)

Legend:
- Departing
- Cruisng
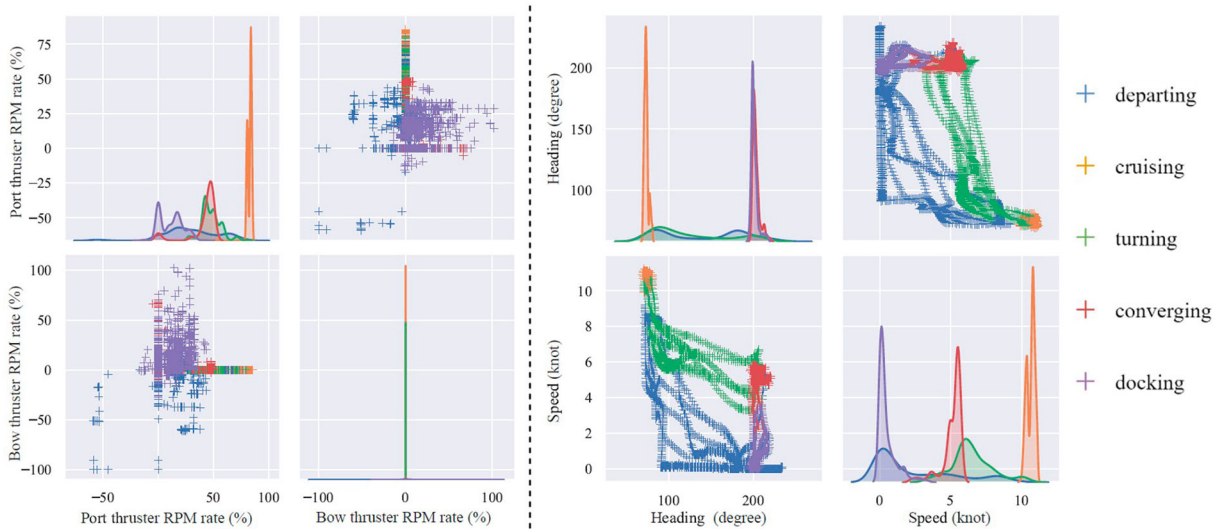- Turning
- Converging
- Docking

**Figure 3.** Selected pair plots. (This figure is available in colour online.)

Hold-out validation (Berrar 2019). Since we collected 16 sailings' log data, this process can be illustrated as in Table 2. In Table 2, Classifiers 1–15 represent 15 different classifiers train with 1–15 training sets (for example, a possible training-set combination for Classifier 3 could be Sailing dataset No. 1, 2 and 3 or any other combinations of three sailing datasets), while test sets 1–16 mean No. 1–16 sailing datasets (single sailing dataset).

### 2.5. Likelihood map and safety level calculation

As log data accumulated along the sailings run times by times, the database for training the SVM classifier is getting larger. Besides the eight featured data items, the geographical information is also recorded. Therefore, another database can be constructed based on the geographical information of those data points which are correctly classified by the classifier. And data points can be drawn on a geographical map reflecting the site of each scenario in the sailing route. Then the map can be converted into a heat map in terms of the density of the geographical distribution of data points. At this step, kernel density estimation method helps to calculate the estimated density at each datum point $x_j$:

$$\hat{p}(x_j) = \frac{1}{mh} \sum_{i=1}^{m} K(\frac{x_j - x_i}{h}) \tag{6}$$

**Table 2.** Illustration of the classifier evolution process.

| | Classifier | | | |
|---|---|---|---|---|
| Testset | 1 | 2 | … | 15 |
| 1 | – | – | – | – |
| 2 | * | – | – | – |
| … | * | * | … | – |
| 15 | * | * | * | – |
| 16 | * | * | * | * |
| Mean value | * | * | * | * |

*represents a numeric value; – represents no calculation.

where $h$ ($h > 0$) is a smoothing parameter; $K$ is the kernel for scaling, and Gaussian kernel is chosen in this paper to estimate the density. Then a 2D heat map illustrating the density distribution can be drawn accordingly. Since the database is updated after new sailing data are appended, the numerical value of the density will become larger and larger, which implies that raw density value itself does not contain standard useful information to help the human to make decision. Therefore, to avoid it from being nothing but fancy, we normalise the density scale into [0, 1]:

$$\hat{p}_N(x_j) = \frac{\hat{p}(x_j) - \min(\hat{p})}{\max(\hat{p}) - \min(\hat{p})} \tag{7}$$

After the normalisation, the density will always be in a certain scale and in a manner that we explicitly understand: the normalised density 1 refers to the densest site on the sailing route, while 0 refers to the sparsest site. The ferry is believed to be safer when travelling on a site where the normalised density is higher, while the captain should be vigilant when the ferry goes into the low normalised density site. Meanwhile, heat maps can be converted to contours by an interpolation operation based on the normalised density distribution. In this paper, we choose the cubic spline interpolation method to realise this conversion. Then the map is gridded, and the density is calculated by the interpolation. By connecting grid points with the same density value, the contour map is obtained to demonstrate continuous approximation of the density distribution at the vicinity area of the scenario. The distribution function SL($y$) can be obtained by ploy-fitting the statistics of the safety level, where $y$ represents the position.

### 2.6. Verification of how the safety level benefits in MPC

In this part, the concept of safety level is integrated into the cost function to implement the MPC. The control scheme is illustrated as in Figure 4. The vessel kinematics can be

represented as Equation (8). Since we do not consider environment loads at this stage, the right-hand side of the kinetic equation $\tau$ is the input force which equals $[f_u\ f_v\ t_r]'$. $\eta$ is the pose vector as $[N\ E\ \psi]'$. $R(\psi)$ is the horizontal plane rotation matrix in terms of the yaw angle $\psi$. $M$ is the system inertia matrix. $C(v)$ is the Coriolis-centripetal matrix. $D(v)$ is the damping matrix. $H$ equals $[1\ 0\ 0;\ 0\ 1\ 0]$, and $y$ equals $[N\ E]'$.

$$\dot{\eta} = R(\psi)v$$
$$M\dot{v} + C(v)v + D(v)v = \tau \qquad (8)$$
$$y = H\eta$$

The original cost function is defined as follows:

$$J(t) = (y(t+1) - y_{\text{ref}})^T Q(y(t+1) - y_{\text{ref}})$$
$$+ \Delta u(t+1)^T R\Delta u(t+1) \qquad (9)$$

The optimisation goal is to minimise the cost function $J$; we use the positive term $(1 - \text{SL}(y))$ to conform to the implication of safety level and the optimisation target. The cost function is thus augmented as follows:

$$J^*(t) = (y(t+1) - y_{\text{ref}})^T Q(y(t+1) - y_{\text{ref}})$$
$$+ \Delta u(t+1)^T R\Delta u(t+1) + W(1 - \text{SL}(y(t+1))) \qquad (10)$$

Equations (9) and (10) give the cost function at one time-step prediction, while MPC is predicting over a length of time horizon $N_p$ to determine the best control candidate, so the overall cost prediction at a certain time step can be represented as Equation (11).

$$J^*(t) = \sum_{k=t+1}^{t+N_p} J^*(k) \qquad (11)$$

The sailing with the least MSL, among 16 historical sailings, is selected as the reference to carry out the path following task. Comparison will be made between the simulations with different cost functions to verify the effect of the safety level term.

## 2.7. Assessing the safety level by the contour map

At the last step in the proposed method, we establish a concept of safety levels with respect to the normalised density distribution described by contour maps. Safety levels (SL) are directly represented by the normalised density of the geographical location. Hereupon, two dimensionless items can be further calculated to reflect different aims of evaluation: receding safety level (RSL) expressed as Equation (12) and mean safety level (MSL) as Equation (13).

$$\text{RSL}(t) = \frac{\sum\limits_{N(t-\Delta T)}^{N(t)} p_i}{\Delta T} \qquad (12)$$

$$\text{MSL}(t) = \frac{\sum\limits_{i=0}^{N(t)} p_i}{N(t)} \qquad (13)$$

$N$ is the number of accumulated log data points until the moment $t$. $\Delta T$ is the number of sampled data points in the receding horizon, while the receding horizon is chosen manually.

RSL calculates the mean safety level in a fixed time scale. The receding horizon for calculation is updated after each sampling. MSL calculates the mean safety level from the start to current moment $t$. MSL may reflect the overall safety level; hence, it can be used to evaluate the performance of the human manoeuvring in a sailing.

## 3. Results

The proposed method is implemented to the database built upon collected 16 sailings' log data. In this section, results are presented in three parts: classification results from the SVM classifier; the derived likelihood heat maps and normalised numerical contour maps, and online testing. To make the demonstration of the results and the corresponding visualisation more comprehensible, result figures will be partially demonstrated. While the selection of figures is unbiased, it is believed that they are able to reflect the global performance.

### 3.1. Classification result

According to Section 2.4 and Table 2, the classifier is built once the first sailing's log data is added to the SVM training database. As the database evolves when new log data come into, the classifier will be updated therewith. The demonstration of the evolution result irrespective of scenarios is shown as Table 3 and Figure 5.
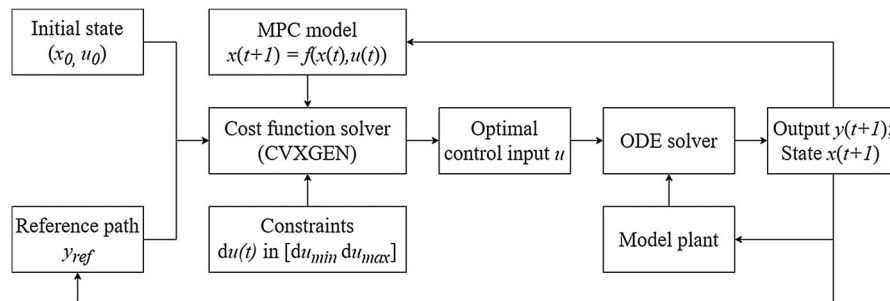


**Figure 4.** Flowchart of the MPC control scheme. (This figure is available in colour online.)

Table 3 shows that the precision of the classification result is increasing as the classifier evolves. While in Figure 5, the precision plunges at the early stage and then rises back rapidly. The diversity between datasets collected from different sailings may account for it, since it is difficult to make an entirely correct description of another sailing by a classifier only trained by very few sailing datasets (one or two). However, after four sailings' log data are added into the database, the classifier can almost guarantee a precision over 90%. As the database is larger, the precision of the classifier keeps growing. At last, the mean value of the classification precision has been developed over 96% based on whole collected sailings' data.

After illustrating the result in a macro-scope, Figure 6 shows the classification precision with respect to different scenarios, and it comprehensively reveals how different scenarios correlate pairwise. In Figure 6, the labels are abbreviated: DPT for departing; CRS for cruising; TRN for turning; CVG

for converging and DCK for docking. From CLF No. 4 to No. 9, the evolution improves its predicting capacity on CVG scenario significantly, but the classifier incorrectly predicts many TRN data points as CVG, which results in the declination of the prediction precision on TRN. Meanwhile, the prediction precision on DCK also grows slightly. Then by comparing the latter two, it shows that the predicting precision is improved remarkably on DPT from 84% to 90%. However, the same problem occurs again that the prediction precision on CVG continues to grow on sacrifice of the declination on TRN, in a moderate manner. In general, the performance of the classifier is improved after several evolutions.

### 3.2. Likelihood heat maps and derived contours

According to the method introduced in Section 2.4, heat maps, based on the accumulated database, can be drawn, as shown in Figure 7. The first five subplots show the heat map of each scenario, while the last subplot at the right bottom shows an overview of the complete route.

The heat maps can help the reader, for example, captains have a direct sense of the most travelled sites. And this feature is prominent especially in scenarios cruising, turning, and converging. However, since both the departing and docking are

**Table 3.** Illustration of the classifier evolution process.

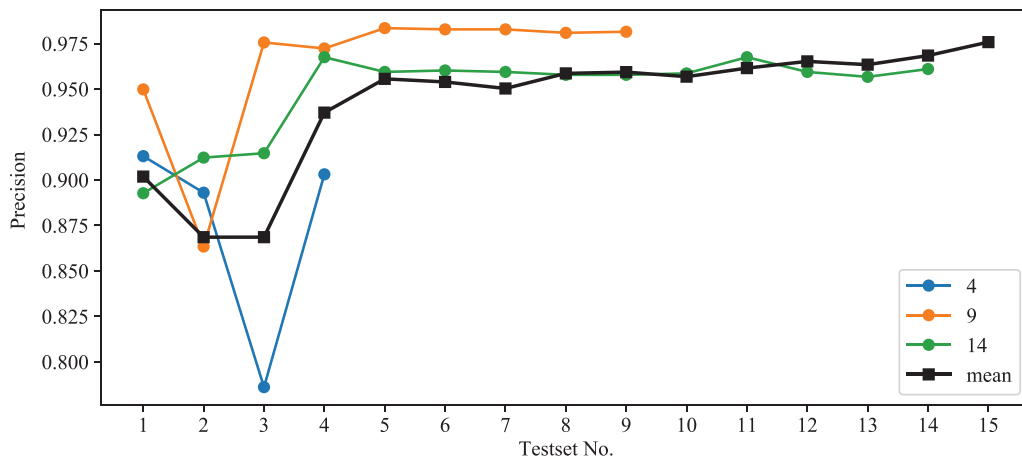| Testset | Classifier | | |
|---|---|---|---|
| | 4 | 9 | 14 |
| 5 | 0.9031 | – | – |
| 10 | 0.9723 | 0.9815 | – |
| 15 | 0.9675 | 0.9578 | 0.9610 |
| Mean value | 0.9370 | 0.9593 | 0.9684 |



**Figure 5.** Evolution of the classifier according to Table 2. (This figure is available in colour online.)
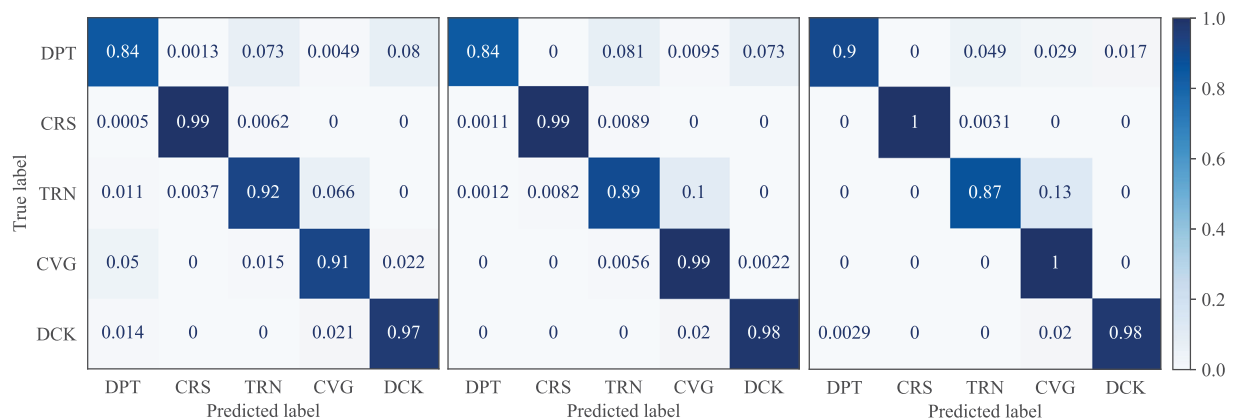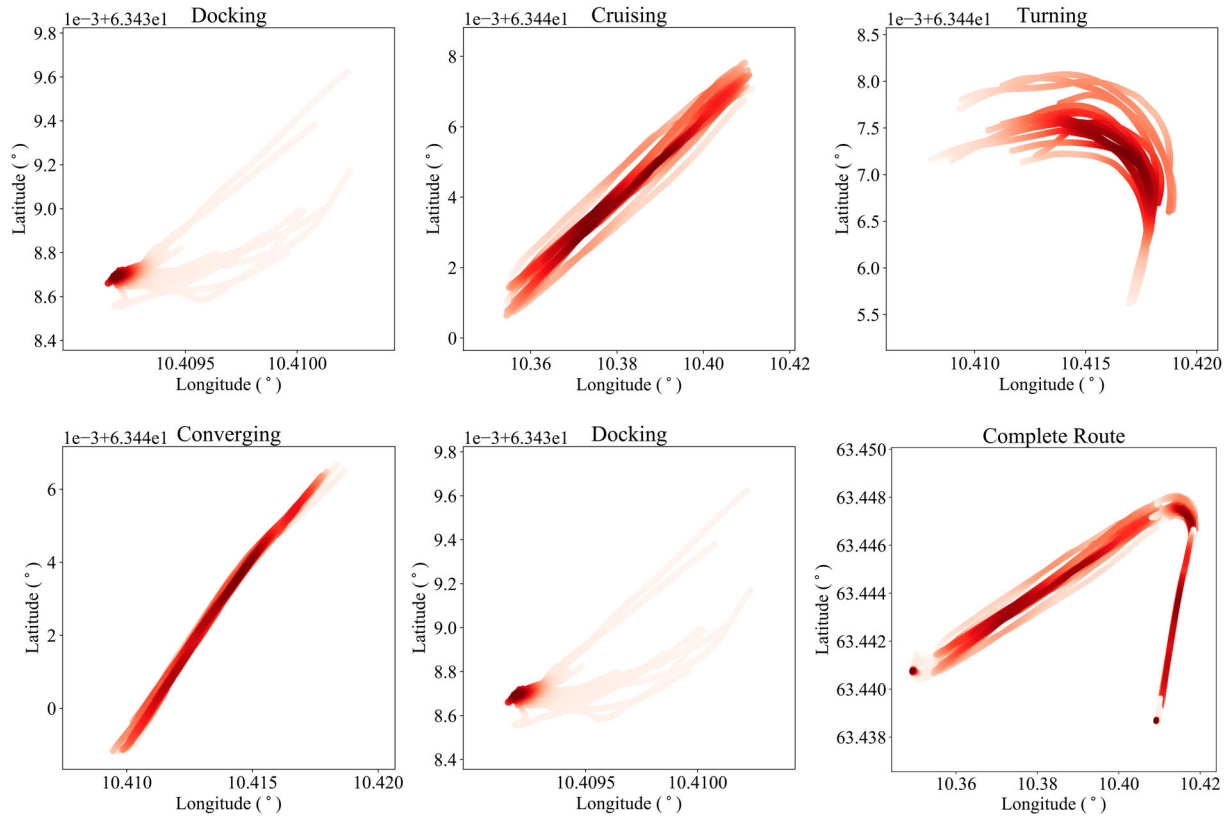


**Figure 6.** Confusion matrix reflecting precision by scenarios (left: CLF No.4; middle: CLF No. 9; right: CLF No. 14). (This figure is available in colour online.)

**Figure 7.** Heat maps of different scenarios. (This figure is available in colour online.)

undergoing in a very concentrated site, the density distribution appears to be somewhat diffusion. However, it is thought to be in a tolerant extent, and can be ameliorated as the database is larger.

Based on heat maps shown in Figure 7, a set of contours with respect to each scenario can be drawn as Figure 8. Different from the heat maps that provide an intuitive illustration and sense of the most travelled area, the set of contours quantitatively demonstrates how the density distributes on a geographical map. Since contours are obtained by an interpolation operation, its fidelity and creditability are dependent on the quantity of data. In general, the overall trend in each scenario has been shown. For example, in the contour of cruising scenario – the closer to the centre of the heat area, the larger the normalised density.

### 3.3. Accumulative manoeuvring knowledge for on-board decision support

As the sailing data are classified by SVM (in Section 2.4) and the results are obtained (in Section 3.1), informative statistics on how captains manoeuvre the ferry during different scenarios are made as in Table 4.

Bow thruster is only turned on during departing and docking when a side force is needed to push the ferry into/out the quay. The behaviours of port- and star-thruster are almost in the same scale, except for the azimuth angle during docking scenario. It depends on which side the ferry docks since solely adjusting the azimuth angle of the outer thruster is able to balance the torque generated at the bow thrust. Since in

this commuting route, the ferry docks at its star-board side (e.g. the coastal to its right), the port-thruster becomes the outer thruster so that its azimuth angle is adjusted as required.

Since the calculated safety levels MSL and RSL are returned to the captain in real time, when the calculated safety levels are falling down to a certain extent, the captain can inspect his manoeuvring commands according to the accumulative manoeuvring knowledge to help him regulate the ferry running in a correct status.

### 3.4. Verification in the MPC loop

In this part, the path following simulation results will be shown and assessed. Figure 9 shows the path of reference (Sailing No. 6), the original MPC and the improved MPC with safety level (MPC-SL). The safety level assessment is given as Table 5. The prediction horizon $N_p$ in MPC and MPC-SL is set as 10.

It should be emphasised that the way how we evaluate the control performance shown in Figure 9 is slightly different from the traditional approach. Traditionally, we balance the input cost and the error reduction to have an optimal solution. In addition to those two items, we augment the cost function with a safety level SL($y$) factor, as in Equation (10). Then it becomes a balance among these three dimensions. Besides having an acceptable reference path following, it requires to have a better safety level evaluation, which is shown in Table 5 in detail.

From the safety level statistics in Table 5, we can implicitly summarise that the safety level has a strong impact on the
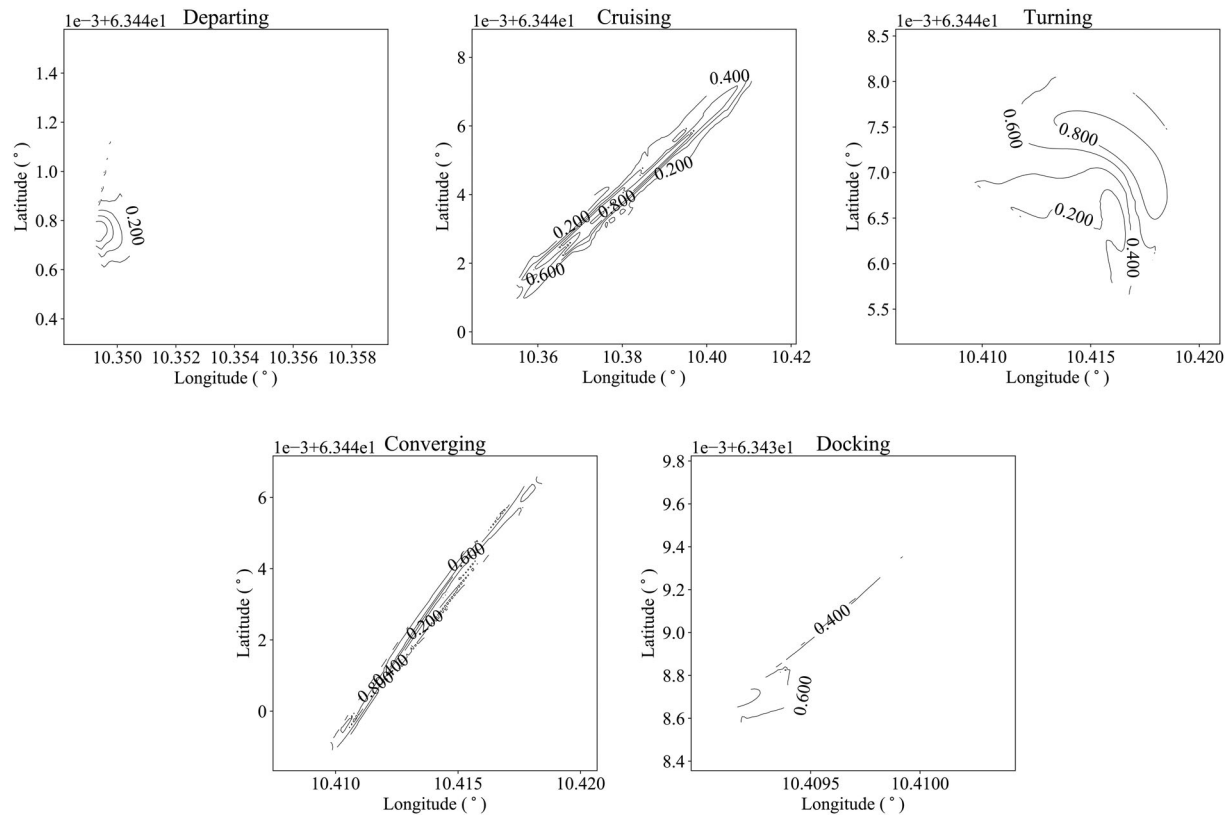
**Figure 8.** Contour of different scenarios. (This figure is available in colour online.)

**Table 4.** On-board machinery status in different scenarios.

| Actuator | DPT | CRS | TRN | CVG | DCK |
|---|---|---|---|---|---|
| Bow-thruster (%) | >0.1 | – | – | – | >10 |
| Port-RPM (%) | <60 | >75 | [40, 60] | [40, 60] | [0, 30] |
| Star-RPM (%) | <60 | >75 | [40, 60] | [40, 60] | [0, 30] |
| Port-azimuth (°) | >0.5 | <1 | >0.5 | <2 | >50 |
| Star-azimuth (°) | >0.5 | <1 | >0.5 | <2 | <1 |

control. After the safety level term is added into the cost function, the overall safety level increases significantly, and so as in scenarios DPT, CRS and TRN.

When the vessel travels in a narrow water tunnel in CVG, where the gradient of the safety level can be very sharp, the safety level suffers a decline but in a moderate level. When the vessel is in the final bow thrusting stage, where the safety
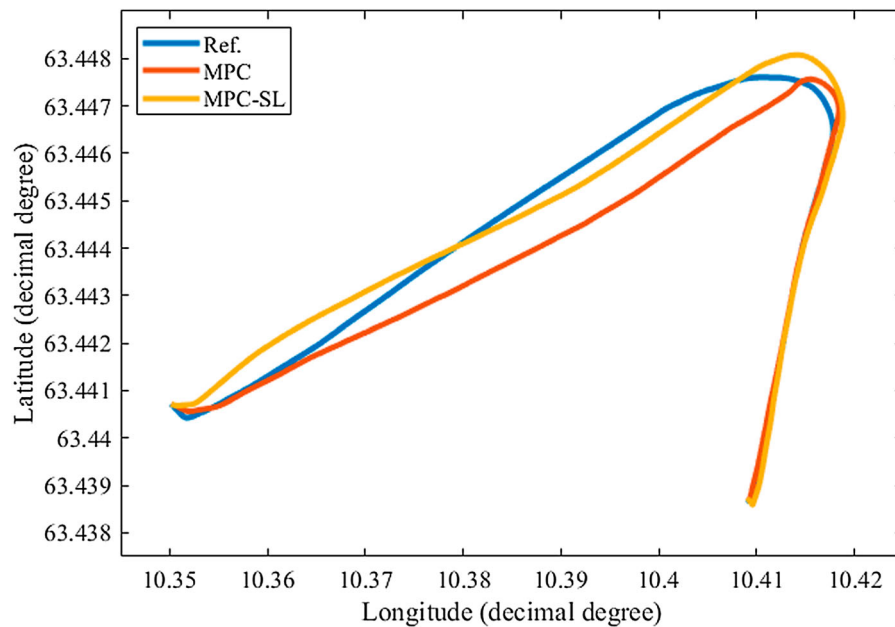


**Figure 9.** Path following simulation by MPC (the path corresponds to Figure 1). (This figure is available in colour online.)

**Table 5.** Illustration of the classifier evolution process.

| Scenario | Safety level | | |
| --- | --- | --- | --- |
| | Ref. | MPC | MPC-SL |
| DPT | 0.4203 | 0.4574 | **0.5449** |
| CRS | 0.4259 | 0.5135 | **0.6743** |
| TRN | 0.6851 | 0.6304 | **0.6999** |
| CVG | 0.5065 | **0.5938** | 0.5059 |
| DCK | **0.6161** | 0.4157 | 0.4158 |
| Overall | 0.5199 | 0.4574 | 0.5681 |

level heat map almost concentrates on a point, it is difficult for the vessel to be strictly in the circle of high safety so that the safety level in DCK is low. In general, the safety level term improves the control in terms of safety noticeably, which suggests that the proposed methodology attains a good performance and further study can be conducted in practice.

## 3.5. Safety level assessment

In this part, safety level assessments are conducted from two aspects. One is sailing status recognition for a whole sailing dataset, and another is safety level evaluation.

Figure 10 shows the result of the online sailing status recognition testing. The dashed lines divide the timeline into segments remarking real periods of each scenario, while the mark '+' represents the recognised status at each sampling step. There are two wild points in the DPT stage, where the sampled data are incorrectly recognised as DCK and TRN. The problem occurs mainly at the TRN stage, where the classifier improperly recognises the ferry to enter the next stage ahead of the real situation, which may be resulted from the similarity between the manoeuvring operations during the late phase in TRN and the early phase in CVG. The classifier has a good performance in judging CRS and DCK during the online testing.

According to the defined terms in Section 2.7 and the obtained contour maps, safety level evaluation is implemented accordingly. The real-time safety level at each sampling step is represented by diluted lines in Figure 11. Firstly, it should be mentioned that since contour maps are derived for each scenario separately and are not merged into one ensemble, the safety level evaluation experiences a gap when the ferry transits between two scenarios. Secondly, it is notable that, excluding
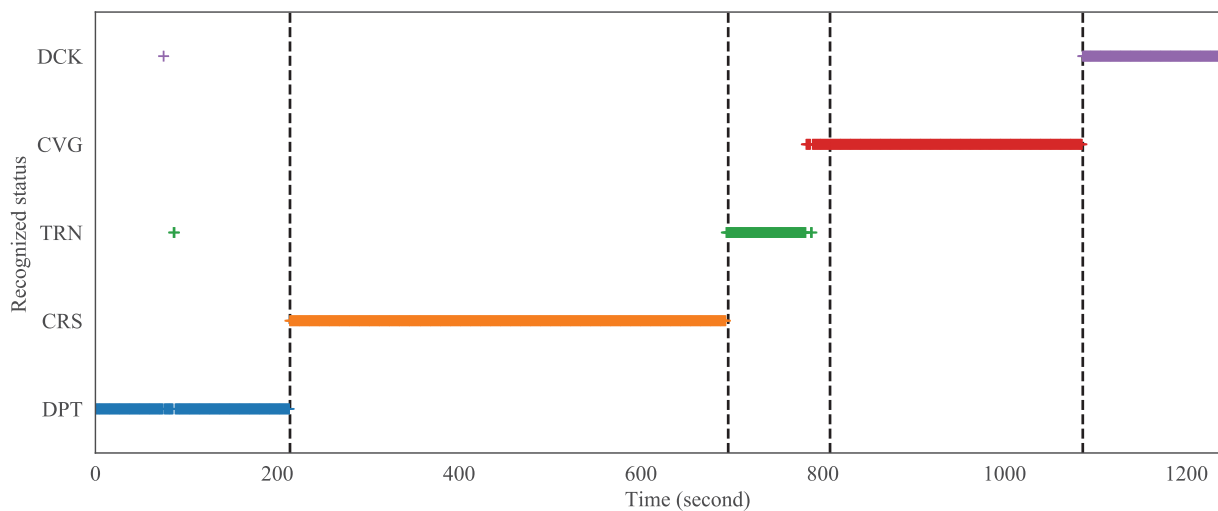


**Figure 10.** Online testing of the sailing status recognition. (This figure is available in colour online.)
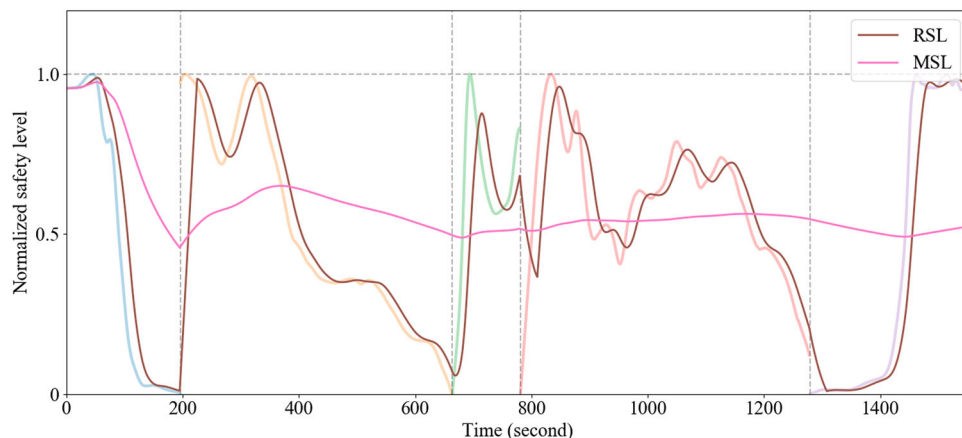


**Figure 11.** Calculated MSL and RSL (diluted lines are the real-time safe level). (This figure is available in colour online.)

the start and the end stage of the whole sailing, the safety level is usually low at the start and end of each single scenario. It may be explained according to the distribution shown in Figure 7. In those heat maps, there is a conspicuous high-density area in each scenario, while at the start and the end, the distribution inclines to disperse, which consequently results in the decline of the safety level at the marginal area.

According to Section 2.7, the two items MSL and RSL, reflecting the safety level from different aspects, are calculated, and shown as in Figure 11. Since RSL calculates the average safety level at a fixed length of the past period, there is a delay to reflect the change of the safety level. This delay provides RSL the ability to reduce the effect at the start and the end during the transition time between different scenarios, which makes RSL to describe the sailing safety in a moderate way. Since critical operations are expected to be taken at the transition period between two scenarios, RSL drastically decreases to a low level to reflect the high possibility of committing a mistake during the transition. MSL demonstrate the safety level with a global insight. It is noticed that because of the long-term steady sailing of the ferry, there is a swell of the safety level during both CRS and CVG scenarios. At last, MSL can provide an overall evaluation of the sailing safety.

RSL and MSL reflect the safety level from two aspects based on the constructed safety level contour maps by a numerical judgement explicitly. It provides an intuitive and quantitative approach for the captain to take the advantage of the knowledge accumulated on this commuting route.

## 4. Conclusion

This paper introduces a method to utilise log data from a ferry to establish an on-board safety awareness system in order to help humans to make decisions. Successful sailings are still thought to be a good paradigm for both designing autonomous ferries and evaluating the manoeuvre quality of every sailing. Hence, we split a customised sailing route and define different scenarios in favour of the human expertise. Collected data are classified by an SVM algorithm and its results are presented as figures of heat maps and contours by the statistical method. Both sets of figures together may assist to evaluate the sailing safety level. Since the ferry may deviate from the designated path no matter under human operations or under autonomous manoeuvring, the figures give a set of metrics to qualitatively and quantitatively know whether the current situation is safe or not, based on the past experience which is reflected by historical log data. By defining new items reflecting safety levels with respect to geographical locations, the result can be used to optimise the control. MPC is designed with the safety level term integrated to verify its significance. From the simulation results, the safety level has a great impact on and ameliorates the control loop. From this research work, we suggest a framework how log data can be comprehensively used to provide on-board support and enhance the sailing route safety. The main idea in this paper is to synthetically use both human expertise and objective log data to make rudiment work for autonomous navigation. It is also under a grand framework that we aim to achieve reliable on-board decision support and ship autonomy by finding, interpreting, learning, and imitating the captains' operating behaviours. For the future work, first, since the log data collected in this paper are from only one commuting route in moderate environment conditions, log data from other commuting routes and types of weather windows should be collected and analysed to examine the universality of the proposed method; second, further study can be focused on the sensitivity of the safety level to the gradient in terms of geographic distance to optimise the control performance.

## Disclosure statement

No potential conflict of interest was reported by the author(s).

## ORCID

*Baiheng Wu* 🆔 http://orcid.org/0000-0002-1824-6784
*Guoyuan Li* 🆔 http://orcid.org/0000-0001-7553-0899
*Hans Petter Hildre* 🆔 http://orcid.org/0000-0003-1444-7818
*Houxiang Zhang* 🆔 http://orcid.org/0000-0003-0122-0964

## References

Aly M. 2005. Survey on multiclass classification methods. Neural Netw. 19:1–9.

Berrar D. 2019. Cross-validation. Encycl Bioinform Comput Biol. 1:542–545.

Borkowski P. 2012. Data fusion in a navigational decision support system on a sea-going vessel. Pol Marit Res. 19(4):78–85.

Calabrese F, Corallo A, Margherita A, Zizzari AA. 2012. A knowledge-based decision support system for shipboard damage control. Expert Syst Appl. 39(9):8204–8211.

Chauvin C, Clostermann JP, Hoc J-M. 2008. Situation awareness and the decision-making process in a dynamic situation: avoiding collisions at sea. J Cogn Eng Decis Mak. 2(1):1–23.

Elkins L, Sellers D, Monach WR. 2010. The autonomous maritime navigation (AMN) project: field tests, autonomous and cooperative behaviors, data fusion, sensors, and vehicles. J Field Robot. 27(6):790–818.

Fossdal M. 2018. Online consequence analysis of situational awareness for autonomous vehicles [master's thesis]. NTNU.

Hagen IB, Kufoalor DKM, Brekke EF, Johansen TA. 2018. MPC-based collision avoidance strategy for existing marine vessel guidance systems. 2018 IEEE International Conference on Robotics and Automation (ICRA). IEEE; p. 7618–7623.

Islam R, Yu H, Abbassi R, Garaniya V, Khan F. 2017. Development of a monograph for human error likelihood assessment in marine operations. Saf Sci. 91:33–39.

Lazarowska A. 2012. Decision support system for collision avoidance at sea. Pol Marit Res. 19(Special):19–24.

Li G, Lai W, Sui X, Li X, Qu X, Zhang T, Li Y. 2020. Influence of traffic congestion on driver behavior in post-congestion driving. Accid Anal Prev. 141:105508.

Li G, Li SE, Cheng B, Green P. 2017. Estimation of driving style in naturalistic highway traffic using maneuver transition probabilities. Transp Res C Emerg Technol. 74:113–125.

Li G, Mao R, Hildre HP, Zhang H. 2019. Visual attention assessment for expert-in-the-loop training in a maritime operation simulator. IEEE Trans Ind Inf. 16(1):522–531.

Li G, Wang Y, Zhu F, Sui X, Wang N, Qu X, Green P. 2019b. Drivers' visual scanning behavior at signalized and unsignalized intersections: a naturalistic driving study in China. J Saf Res. 71:219–229.

Li G, Zhu F, Qu X, Cheng B, Li S, Green P. 2019a. Driving style classification based on driving operational pictures. IEEE Access. 7:90180–90189.

Maaten LVD, Hinton G. 2008. Visualizing data using t-SNE. J Mach Learn Res. 9(Nov):2579–2605.

Nielsen UD, Jensen JJ. 2011. A novel approach for navigational guidance of ships using onboard monitoring systems. Ocean Eng. 38(2-3):444–455.

Nilsson M, Van Laere J, Ziemke T, Edlund J. 2008. Extracting rules from expert operators to support situation awareness in maritime surveillance. 2008 11th International Conference on Information Fusion; Jun. IEEE; p. 1–8.

Nisizaki C. 2019. Onboard measurements of navigator's situation awareness in congested sea area. 2019 IEEE International Conference on Systems, Man and Cybernetics (SMC); Oct. IEEE; p. 4296–4301.

Perera LPH, Rodrigues JMJD, Pascoal R, Soares CG. 2012. Development of an onboard decision support system for ship navigation under rough weather conditions. In: E. Rizzuto, C. Guedes Soares, editors. Sustainable maritime transportation and exploitation of sea resources. London, UK: Taylor & Francis Group; p. 837–844.

Pietrzykowski Z, Magaj J, Wołejsza P, Chomski J. 2010. Fuzzy logic in the navigational decision support process onboard a sea-going vessel. International Conference on Artificial Intelligence and Soft Computing; Jun. Berlin: Springer; p. 185–193.

Pietrzykowski Z, Wołejsza P, Borkowski P. 2017. Decision support in collision situations at sea. J Navig. 70(3):447–464.

Ren Z, Han X, Verma AS, Dirdal JA, Skjetne R. 2021. Sea state estimation based on vessel motion responses: Improved smoothness and robustness using Bézier surface and L1 optimization. Marine Structures. 76: 102904.

Simsir U, Amasyalı MF, Bal M, Çelebi UB, Ertugrul S. 2014. Decision support system for collision avoidance of vessels. Appl Soft Comput. 25:369–378.

Tengesdal T, Brekke EF, Johansen TA. On collision risk assessment for autonomous ships using scenario-based MPC.

TøNdel P, Johansen TA, Bemporad A. 2003. An algorithm for multi-parametric quadratic programming and explicit MPC solutions. Automatica (Oxf). 39(3):489–497.

Vettor R, Soares CG. 2015. Multi-objective route optimization for onboard decision support system. In: Weintrit A, Neumann T, editors. Information, communication and environment: marine navigation and safety of sea transportation. Leiden: CRC Press, Taylor & Francis; p. 99–106.

Wiegmann DA, Shappell SA. 2017. A human error approach to aviation accident analysis: the human factors analysis and classification system. London, UK: Routledge.

Wu B, Li G, Zhao L, Hildre HP, Zhang H. 2020. A human-expertise based statistical method for analysis of log data from a commuter ferry. 2020 15th IEEE Conference on Industrial Electronics and Applications (ICIEA); Nov. IEEE; p. 1471–1477.

Xu H, Rong H, Soares CG. 2019. Use of AIS data for guidance and control of path-following autonomous vessels. Ocean Eng. 194: 106635.

Zhang L, Meng Q, Xiao Z, Fu X. 2018. A novel ship trajectory reconstruction approach using AIS data. Ocean Eng. 159:165–174.